Ferenc Tajti, Géza Szayer, Bence Kovács, Péter Barna, Péter Korondi

Optical flow based odometry for mobile robots supported by multiple sensors and sensor fusion

This paper introduces an optical flow based odometry solution for indoor mobile robots. The indoor localization of mobile robots is an important issue according to the increasing mobile robot market and the needs of the industrial, service and consumer electronics sectors. The robot odometry calculated from the robot kinematics accumulates the position error caused by the wheel slip but an optical flow based measurement is independent from wheel slipping so both methods have different credibility which was considered during the sensor fusion and the development. The focus of the research was to design an embedded system with high accuracy on the possibly lowest price to serve the needs of the consumer electronics sector without the need of expensive camera and real-time embedded computer based high level robot localization solutions. The paper proposes the theoretical background, the implementation and the experimental results as well. The universal optical flow module can be implemented in any kind of indoor mobile robot to measure the position and the orientation of the robot during the motion, even in the case of a 3 DoF holonomic drive like kiwi drive. The application of omnidirectional wheels in mobile robotics requires high accurate position and orientation feedback methods contrary to differential drives.

Key words: Mobile robot, Omni drive, Odometry, Optical flow, Sensor correlation

Odometrija mobilnog robota zasnovana na optičkom toku podržana s više senzora i fuzijom senzora. Ovaj rad predstavlja rješenje odometrije mobilnog robota za unutrašnje prostore koje se zasniva na optičkom toku. Lokalizacija mobilnog robota u unutrašnjim prostorima je veoma važno pitanje u rastućem tržištu mobilnih robota i potreba industrijskog, uslužnog i sektora potrošačke elektronike. Odometrija robota izračunata iz kinematike robota nakuplja greške s vremenom radi sklizanja kotača, dok na odometriju izmjerenu optičkim tokom klizanje ne utječe, te obje metode imaju različit kredibilitet što je uzeto u obzir prilikom fuzije senzora i razvoja. Fokus istraživanja je bio dizajnirati ugradbeno sustav visoke točnosti i niske cijene koji bi zadovoljio potrebe sektora potrošačke elektronike bez potrebe za skupim kamerama i lokalizacijskim rješenjima mobilnog robota visokog nivoa namijenjenim izvođenju na ugradbenim računalima za rad u stvarnom vremenu. U radu je iznesena teorijska podloga, implementacija i eksperimentalni rezultati. Univerzalni modul za izračun optičkog toka može se implementirati na bilo kojem mobilnom robotu za unutrašnje prostore kako bi mjerio poziciju i rotaciju robota tijekom gibanja, čak i u slučaju 3 DoF holonomskog pogona kao što je kiwi pogon. Korištenje svesmjernih kotača u mobilnoj robotici zahtjeva visoku točnost pozicije i orijentacije za razliku od diferencijalnog pogona.

Ključne riječi: Mobilni robot, Svesmjerni pogon, Odometrija, Optički tok, Korelacija senzora

1 INTRODUCTION

The need for automation and robotics solutions is an everyday topic in the industrial sector. There is also a growing need in daily life situations, such as floor cleaning, lawn moving, window cleaning and other things solvable by mobile robotics. The motion in an indoor or an outdoor environment is the most important task of a mobile robot, which is impossible without appropriate localization. The required accuracy of the robot position and orientation is usually defined by the application. The accuracy requirements are different in case of outdoor and indoor mobile robots, where the travel distance is also different. As an example, 2 meters inaccuracy is acceptable during a 250 meters quad copter flight, but in case of an indoor robot the width of a corridor can be only 2 meters. For indoor localization, several vision and kinematics based methods and applications exist like [1, 2]. The kinematics based solution calculates the robot position and orientation from the angular position of the wheels, which accumulates the error according to the slippery floor [3-6]. The vision based methods requires embedded computers or normal external PC-s to provide enough calculation throughput for the al-

gorithms [7]. Our solution for the improvement of wheel based odometry is an optical based method with minimal calculation throughput on the lowest price for the mobile robots of the service sector. Service robot usually does not have any kind of embedded computers, but has simple RISK microcontroller based embedded systems. It is also important to mention; that the proposed method does not need the use of any external localization elements, like infra light beacons, ultrasonic sensors, visual markers, etc. In the consumer electronics sector the production of mobile robots should be solved on the possibly lowest variable costs. Difficult software based solutions with cheap hardware elements are beneficial for products manufactured in quantity.

At first this paper describes the control problems of omnidirectional mobile robots. In the next section three methods are proposed for measuring position and orientation. Section 3 describes the odometry based methods. Section 4 describes the fusion of the results given from the different methods, then section 5 describes the open loop test results. Finally, section 6 concludes the paper.

2   ODOMETRY INACCURACY

In the view of the motion on the ground plane a mobile robot can have 2 or 3 degrees of freedom (DoF) depending on the structure of the drive. In case of 3 DoF (e.g. holonomic drives), the robot can change the position and the orientation at the same time, but a 2 DoF robot (e.g. differential drives) cannot change position and orientation independently. A mobile robot with holonomic drive can also move in any ways on the ground plane without the change of the robot orientation. Holonomic robots have mechanisms to control all 3 physical DoF on the ground plane. Holonomic drives with three omniwheels are also known as kiwi drives. The research was inspired by Ethon (see Fig. 1) [8], which is our self-designed kiwi drive based holonomic mobile robot, made for ethological research. On a slippery floor after 15-30 meters of motion in different directions the odometry of Ethon accumulated 2-5 meter errors in any directions and 10-30° in orientation, which is impermissible. [9] The errors of the position and the orientation come from the following problems:

- the wheels are slipping [10,11]

- the contact points between the wheels and the floor alternate (see Fig. 2)

- the results of the sine and cosine are calculated from a 1° resolution look-up table

- the sine and the cosine functions in the implementation of the inverse kinematics are formulated to tangent functions and estimated with the division of integer numbers
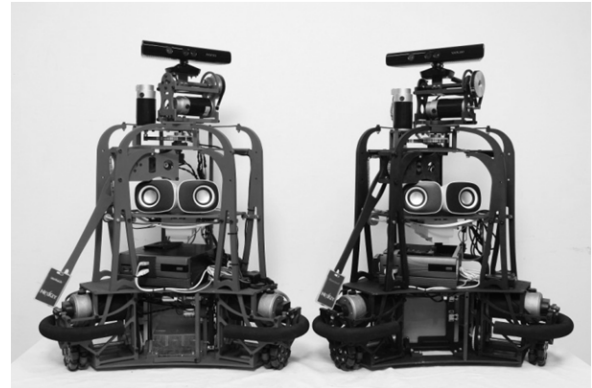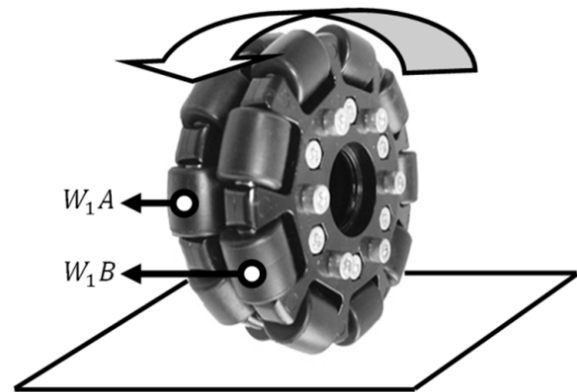

Fig. 1. Ethon robots

Fig. 2. Contact points of an omni wheel

The error related to the contact points (δ_1) is 5.4%, which can be calculated as (1), where $\Delta\left(W_1, W_2\right)$ is the distance between the contact points of wheel 1 and r (the radius of the robot geometry) is the distance between the center of the robot structure and the wheels.

$$\delta_1 = \frac{\Delta\left(W_1, W_2\right)}{r} = \frac{16.2\,[mm]}{300\,[mm]} = 0.054 \qquad (1)$$

The 1° resolution look-up table causes 0.27% error (δ_2). The estimation of the tangent function causes 2.15% error (δ_3). According to the errors ($\delta_1, \delta_2, \delta_3$) and the undefined wheel slipping error (δ_4) the robot accumulates in the worst case about $\pm$5-8 % error. During the measurements at 15 meters of continuous linear driving in the robot position it caused in worst case 0.5-1 meter error. This can be accepted and compensated with the high level mapping localization of the robot. During the measurements of the angular position the $\pm$5-8% position error caused about 10-30° angular error between the robot coordinate system and the world coordinate system. If the robot moves sideways with 10-30° angular error it causes 11-33% position error, which cannot be accepted, because it means 5 meters in a
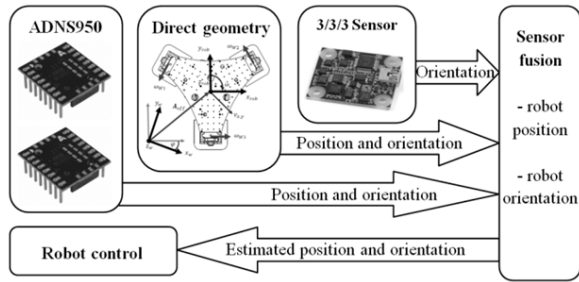
Fig. 3. The sensors on the robot base

15 meter drive. (In case of 90° error the robot changed the x-y directions, which is 100% position error, because sinus 90° = 1.)

3   ODOMETRY METHODS

Mobile robots can be controlled without position and orientation feedback. In this case only the servo amplifiers have their own angular position feedback during the motion and the references of the wheels can be calculated by the equations of the inverse kinematics. For a mobile robot with differential drive, this method provides an appropriate indoor localization. In case of mobile robot drives, where the wheels or tracks slip on the ground more sophisticated control methods are required. To solve the problems of the robot localization three types of measurement methods were implemented and investigated on the robot: 3/3/3 sensor, ADNS9500 optical flow sensors, and inverse geometry. (See Fig. 3.)

3.1   Odometry based on wheel rotation

For the motion control of the robot, both the inverse kinematics and the direct geometry were implemented in the central controller unit of the robot, which provides the wheel references for the servo amplifiers of the robot real-time in 1 kHz via CAN-bus interface. The transformation between the world coordinate system and the robot coordinate system can be described as (2) with one rotational (around axis z) and two linear transformations (along x and y). (See Fig. 4.)

$$T_{W \to R} : \Re^3 \xrightarrow{Rot(z,\varphi)^T \cdot Trans(x,\Delta x)^{-1} \cdot Trans(y,\Delta y)^{-1}} \Re^3$$

(2)

The transformation of a point from world coordinate system to robot coordinate system can be expressed straightforward as (3).

$$P_R = (P_W - \mathbf{A}_{offset}) \cdot Rot(z,\varphi)^{-1}$$ (3)

Where the offset can be expressed as a simple vector (4).

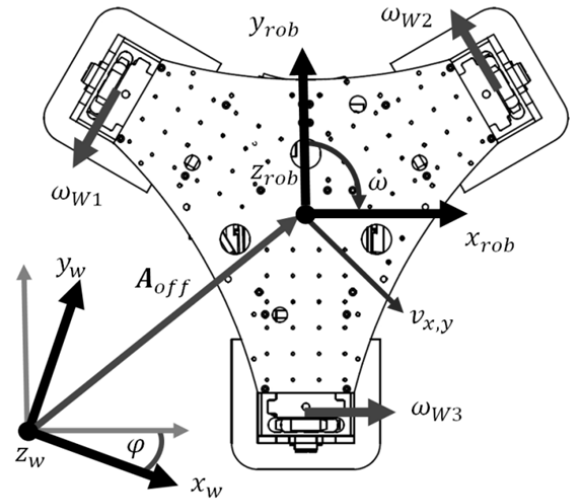$$\mathbf{A}_{offset} = \begin{bmatrix} \Delta x \\ \Delta y \\ 0 \end{bmatrix}$$ (4)

Fig. 4. Robot kinematics

The inverse of the rotation in case of z axis can be expressed as (5).

$$Rot(z,\varphi)^{-1} = \begin{bmatrix} \cos\varphi & \sin\varphi & 0 \\ -\sin\varphi & \cos\varphi & 0 \\ 0 & 0 & 1 \end{bmatrix}$$ (5)

During the implementation of the motion control methods dimensionless integer numbers were used by calculation throughput optimising considerations. The references of the wheels can be expressed from the robot references as (3.5-3.7), where K and C are constants to get real units.

$$\omega_{W1} = K(C \cdot \omega - v_x \cdot \sin 30° - v_y \cdot \cos 30°)$$ (6)

$$\omega_{W2} = K(C \cdot \omega - v_x \cdot \sin 30° + v_y \cdot \cos 30°)$$ (7)

$$\omega_{W3} = K(C \cdot \omega + v_x \cdot 2)$$ (8)

From the equations of the inverse kinematics (3.5-3.7), the equations of the direct geometry can be expressed as (3.8-3.10), where φ_0, x_0, y_0 are the initial position and orientation of the robot and φ, x, y are the actual position and orientation of the robot.

$$\varphi = \int \frac{\omega_{W1} + \omega_{W2} + \omega_{W3} \cdot s30°}{K \cdot C \cdot (s30° + 2)} dt + \omega_0$$ (9)

$$x = \int -\frac{\omega_{W1} + \omega_{W2} - 2 \cdot \omega_{W3}}{2 \cdot K \cdot (s30° + 2)} dt + x_0$$ (10)

$$y = \int -\frac{\omega_{W1} - \omega_{W2}}{2 \cdot K \cdot c30°} dt + y_0$$ (11)

During the robot motion, both the position and the orientation values can be updated externally (for example from
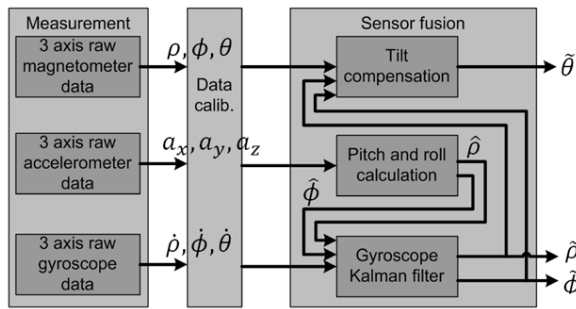
Fig. 5. 3/3/3 sensor block diagram

sensor fusion) in every 50 ms (20 Hz), where at least the orientation should be updated. The motion control of the robot is calculated at 1 kHz, which is 1 ms. According to the maximal velocity (1.5 m/s) and the maximal angular velocity (1.47 rad/s) of the robot the system will not accumlate too much error between two position updates (50 ms) so the motion control can calculate 50 cycles with the values of the inverse geometry functions.

3.2   Gyroscope, accelerometer and magneto sensor

As it is mentioned above, the odometry calculated from equations of the direct geometry accumulated 33% orientation error and only 8% position error. PhidgetSpatial Precision 3/3/3 sensor were used to compensate the orientation problems, which is a measurement card with a 3 axis accelerometer, a 3 axis gyroscope and a 3 axis magnetometer [12]. For PhidgetSpatial Precision 3/3/3 several open source implementations exist. On Ethon, we used sensor fusion with Kalman filter for the gyroscope, pitch and roll calculation and finally tilt compensation to get the angular position value (φ), which is the tilt angle (θ) (see Fig. 5). The measurement card and the implemented method could provide 0.01 radian resolution, which means only 0.16% angular error.

3.3   Optical flow

For the optical flow method we used ADNS9500 gaming mouse sensors, which can measure motion in two directions from 5-10 mm floor height. It is an important fact that different floor surface characteristics influence the measurement. The ADNS9500 sensor measures the surface quality during motion, which can be read from SQUAL sensor register. The maximal value of the register is 169. A white paper can reach around 40 and the register value is nearly equal to zero when there is no surface below the sensor. The value of the SQUAL register was used during the calculation of the optical flow sensor credibility.

The robot has 3 DoF so the system requires two sensors to be able to measure both the robot position and
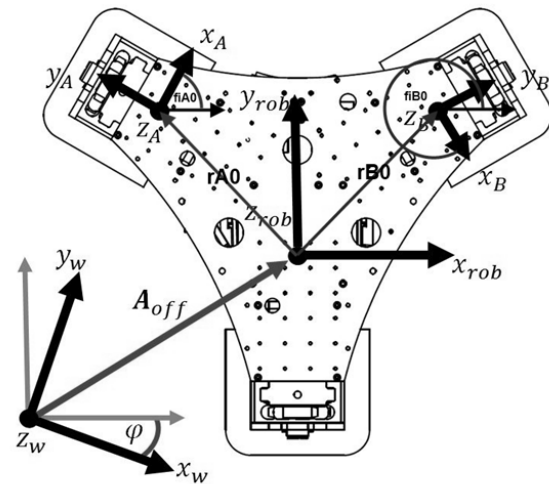

Fig. 6. Optical flow kinematics

orientation [13-15]. Between the sensors and the embedded system we implemented SPI (serial peripheral interface) communications. The position and the orientation of the sensors in robot coordinate system can be described with the following parameters: $x_A, y_A, z_A, r_{A0}, \varphi_{A0}$ and $x_B, y_B, z_B, r_{B0}, \varphi_{B0}$ -as figure 5, where r_{A0}, φ_{A0} and r_{B0}, φ_{B0} are constants. From the optical flow sensors we used only raw data without any ergonomics functions, like mouse acceleration which is usually implemented in computer peripheries. The start of the measurement is synchronized between the sensors in the embedded system and the software updates the absolute x_A, y_A, x_B, y_B and the $\Delta x_A, \Delta y_A, \Delta x_B, \Delta y_B$ values in discrete time so the equations and the implementation of the inverse kinematics [16, 17] are based on these values. (See Fig. 6.) The $\Delta x_A, \Delta y_A, \Delta x_B, \Delta y_B$ parameters of the measurement can be described as (12)-(15).

$$dx_A = dx_w c(\varphi_{A0} + \varphi) + dy_w s(\varphi_{A0} + \varphi) + d\varphi(x_{A0}s\varphi_{A0} - y_{A0}c\varphi_{A0}) \tag{12}$$

$$dy_A = -dx_w s(\varphi_{A0} + \varphi) + dy_w c(\varphi_{A0} + \varphi) + d\varphi(x_{A0}c\varphi_{A0} + y_{A0}s\varphi_{A0}) \tag{13}$$

$$dx_B = dx_w c(\varphi_{B0} + \varphi) + dy_w s(\varphi_{B0} + \varphi) + d\varphi(x_{B0}s\varphi_{B0} - y_{B0}c\varphi_{B0}) \tag{14}$$

$$dy_B = -dx_w s(\varphi_{B0} + \varphi) + dy_w c(\varphi_{B0} + \varphi) + d\varphi(x_{B0}c\varphi_{B0} + y_{A0}s\varphi_{B0} \tag{15}$$

Equations (12)-(15) can be described as (16).

$$
\begin{bmatrix}
c\left(\varphi_{A0}+\varphi\right) & s\left(\varphi_{A0}+\varphi\right) & x_{A0}s\varphi_{A0} - y_{A0}c\varphi_{A0} \\
-s\left(\varphi_{A0}+\varphi\right) & c\left(\varphi_{A0}+\varphi\right) & x_{A0}c\varphi_{A0} + y_{A0}s\varphi_{A0} \\
c\left(\varphi_{B0}+\varphi\right) & s\left(\varphi_{B0}+\varphi\right) & x_{B0}s\varphi_{B0} - y_{B0}c\varphi_{B0} \\
-s\left(\varphi_{B0}+\varphi\right) & c\left(\varphi_{B0}+\varphi\right) & x_{B0}c\varphi_{B0} + y_{A0}s\varphi_{B0}
\end{bmatrix}
$$

$$
\cdot
\begin{bmatrix} dx_w \\ dy_w \\ d\varphi \end{bmatrix}
=
\begin{bmatrix} dx_A \\ dy_A \\ dx_B \\ dy_B \end{bmatrix}
\tag{16}
$$

In this case we measure a 3 DoF system with four parameters, which are not independent and one parameter can be calculated from the others to implement data correlation. The fourth parameter can be expressed from the others generally as (17) and (18).

$$
\mathbf{A} = \begin{bmatrix} x_{A0} - x_{B0} \\ y_{A0} - y_{B0} \end{bmatrix}
\tag{17}
$$

$$
y_B = \frac{x_A \begin{bmatrix} c\varphi_{A0} & s\varphi_{A0} \end{bmatrix} A}{\begin{bmatrix} -s\varphi_{B0} & c\varphi_{B0} \end{bmatrix} A} +
$$
$$
+ \frac{y_A \begin{bmatrix} -s\varphi_{A0} & c\varphi_{A0} \end{bmatrix} A - x_B \begin{bmatrix} c\varphi_{B0} & s\varphi_{B0} \end{bmatrix} A}{\begin{bmatrix} -s\varphi_{B0} & c\varphi_{B0} \end{bmatrix} A}
\tag{18}
$$

In our special case points A and B lie in r_A radius with 120° orientation, where x_A, x_B in the line of the radius and y_A, y_B are perpendicular to the radius. With these conditions y_B can be expressed as (19) and (20).

$$
y_B = \frac{-\frac{1}{2}x_A + \frac{\sqrt{3}}{2}y_A + \frac{1}{2}x_B}{-\frac{\sqrt{3}}{2}}
\tag{19}
$$

$$
y_B = \frac{1}{\sqrt{3}}\left(x_A - x_B\right) - y_A
\tag{20}
$$

According to our special case and $r_{A0}, \varphi_{A0}, r_{B0}, \varphi_{B0}$ constant parameters (16) can be expressed as (22). During the implementation of the system on different robots other simplifications can be made in (16) according to the actual position and orientation of the optical flow sensors in the robot coordinate system.

$$
\begin{bmatrix} dx_A \\ dy_A \\ dx_B \\ dy_B \end{bmatrix}
=
\begin{bmatrix}
c\left(\varphi+\frac{\varphi}{3}\right) & s\left(\varphi+\frac{\varphi}{3}\right) & -r_0 \\
-s\left(\varphi+\frac{\varphi}{3}\right) & c\left(\varphi+\frac{\varphi}{3}\right) & 0 \\
c\left(\varphi+\frac{5\varphi}{3}\right) & s\left(\varphi+\frac{5\varphi}{3}\right) & -r_0 \\
-s\left(\varphi+\frac{5\varphi}{3}\right) & c\left(\varphi+\frac{5\varphi}{3}\right) & 0
\end{bmatrix}
\begin{bmatrix} dx_w \\ dy_w \\ d\varphi \end{bmatrix}
\tag{21}
$$

The pseudo inverse of (21) gives the solution for the Jacobian matrix of the system as (22).

$$
\begin{bmatrix} dx_w \\ dy_w \\ d\varphi \end{bmatrix}
=
$$
$$
\begin{bmatrix}
-\frac{\sqrt{3}s\varphi}{4} & -\frac{4\sqrt{3}c\varphi+3s\varphi}{12} & \frac{\sqrt{3}s\varphi}{4} & \frac{4\sqrt{3}c\varphi-3s\varphi}{12} \\
\frac{\sqrt{3}c\varphi}{4} & \frac{3c\varphi-4\sqrt{3}s\varphi}{12} & -\frac{\sqrt{3}c\varphi}{4} & \frac{3c\varphi+4\sqrt{3}s\varphi}{12} \\
-\frac{1}{2r_0} & -\frac{\sqrt{3}}{6r_0} & -\frac{1}{2r_0} & \frac{\sqrt{3}}{6r_0}
\end{bmatrix}
\begin{bmatrix} dx_A \\ dy_A \\ dx_B \\ dy_B \end{bmatrix}
\tag{22}
$$

In this case the Jacobian matrix can be separated for a rotational matrix around axis z and a transformational matrix on the x-y plane as (23).

$$
\mathbf{J} =
\begin{bmatrix}
c\varphi & -s\varphi & 0 \\
s\varphi & c\varphi & 0 \\
0 & 0 & 1
\end{bmatrix}
\begin{bmatrix}
0 & -\frac{1}{\sqrt{3}} & 0 & \frac{1}{\sqrt{3}} \\
\frac{\sqrt{3}}{4} & \frac{1}{4} & \frac{\sqrt{3}}{4} & \frac{1}{4} \\
-\frac{1}{2r_0} & -\frac{\sqrt{3}}{6r_0} & -\frac{1}{2r_0} & \frac{\sqrt{3}}{6r_0}
\end{bmatrix}
\tag{23}
$$

Equation (23) can be expressed in complex form as (24).

$$
\begin{bmatrix} dx_w + i\, dy_w \\ d\varphi \end{bmatrix}
=
\begin{bmatrix} e^{i\varphi} & 0 \\ 0 & 1 \end{bmatrix} \cdot
$$
$$
\cdot
\begin{bmatrix}
i\frac{\sqrt{3}}{4} & -\frac{1}{\sqrt{3}}+i\frac{1}{4} & i\frac{\sqrt{3}}{4} & \frac{1}{\sqrt{3}}+i\frac{1}{4} \\
-\frac{1}{2r_0} & -\frac{\sqrt{3}}{6r_0} & -\frac{1}{2r_0} & \frac{\sqrt{3}}{6r_0}
\end{bmatrix}
\begin{bmatrix} dx_A \\ dy_A \\ dx_B \\ dy_B \end{bmatrix}
\tag{24}
$$

From (24) the following conclusions can be made:

1. φ (robot orientation) is independent from the length of the path and can be expressed from the actual values of the optical flow sensors

2. to express x, y values (robot position) first the calculation of φ is needed

Simplifying (24) with the value of y_B we can describe the equation as (25).

$$
\begin{bmatrix} dx_w + i\, dy_w \\ d\varphi \end{bmatrix}
=
\begin{bmatrix} e^{-i\frac{x_A+\sqrt{3}y_A+2x_B}{3r_0}} & 0 \\ 0 & 1 \end{bmatrix} \cdot
$$
$$
\cdot
\begin{bmatrix}
\frac{1+i\sqrt{3}}{3} & -\frac{2}{\sqrt{3}} & -\frac{1+i\sqrt{3}}{3} \\
-\frac{1}{3r_0} & -\frac{\sqrt{3}}{3r_0} & -\frac{2}{3r_0}
\end{bmatrix}
\begin{bmatrix} dx_A \\ dy_A \\ dx_B \end{bmatrix}
\tag{25}
$$

From (25) y_w (the y coordinate of the robot position) can be expressed as (26), x_w (the x coordinate of the robot position) can be expressed as (27) and φ (the orientation of the robot) can be expressed as (28).

$$
x_w = \int_0^t \left(\left(\frac{\dot{x}_A}{3} - \frac{2\dot{y}_A}{\sqrt{3}} - \frac{\dot{x}_B}{3}\right) c\left(\frac{x_A+\sqrt{3}y_A+2x_B}{3r_0}\right) + \right.
$$
$$
\left. + \frac{\sqrt{3}}{3}\left(\dot{x}_A - \dot{x}_B\right) s\left(\frac{x_A+\sqrt{3}y_A+2x_B}{3r_0}\right) \right) dt
\tag{26}
$$

$$
y_w = \int_0^t \left(\frac{\sqrt{3}}{3}\left(\dot{x}_A - \dot{x}_B\right) c\left(\frac{x_A+\sqrt{3}y_A+2x_B}{3r_0}\right) - \right.
$$
$$
\left. - \left(\frac{\dot{x}_A}{3} - \frac{2\dot{y}_A}{\sqrt{3}} - \frac{\dot{x}_B}{3}\right) s\left(\frac{x_A+\sqrt{3}y_A+2x_B}{3r_0}\right) \right) dt
\tag{27}
$$

$$
\varphi = -\frac{x_A + \sqrt{3}y_A + 2x_B}{3r_0}
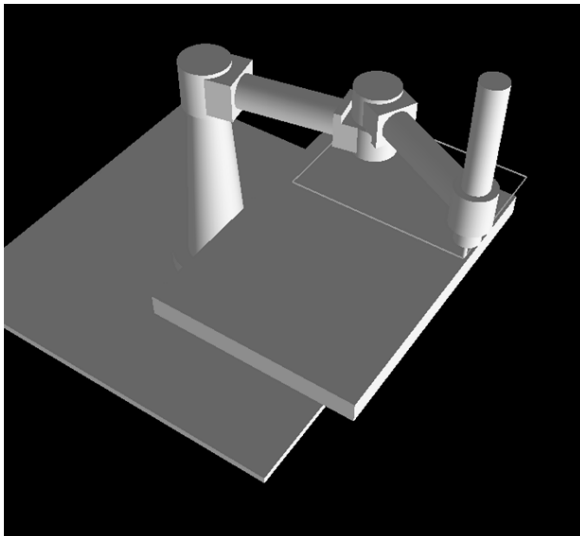\tag{28}
$$

Fig. 7. SCARA measurement 3D

Fig. 8. SCARA measurement

With (26), (27) and (28) the homogenous transformational matrix of the system can be expressed as (29).

$$\mathbf{H} = \begin{bmatrix} c\varphi & -s\varphi & 0 & x_w \\ s\varphi & c\varphi & 0 & y_w \\ 0 & 0 & 1 & 0 \\ 0 & 0 & 0 & 1 \end{bmatrix} \quad (29)$$

For the validation of the equations of the optical flow embedded system we used our open source real-time Linux (and LinuxCNC) based robot controller. During the measurements a SEIKO D-Tran 4400 SC SCARA robot moved the sensor system in 3 DoFs (x, y, φ). The accuracy of the robot is higher with a magnitude than the accuracy of the optical flow system. In case of this robotized validation measurement, the position and the orientation can be modified accurately and the measurement can be repeated. See Fig. 7 and Fig. 8. Refocusing the sensors the method can be improved [18, 19]. The first measurements were made with constant orientation at each point in order to simulate holonomic movement. The grey line on Fig. 9. was the path of the robot, which was plotted from G-code and the dotted black line was measured with the optical flow system. The difference between the lines (the position error) is acceptable (less than 10 mm). During second measurement the orientation was always perpendicular to the direction of motion (like the motion of a mobile robot with differential drive). The grey line represents the path of the robot (plotted from the G-code) and the black dotted line represents the path, which was measured by the optical flow sensors. See Fig. 10. In this case the error is also acceptable (less than 10 mm). The optical flow system measures the motion of its own center point and it could not be fixed to the tool center point (TCP) of the SCARA robot with less than 2-3
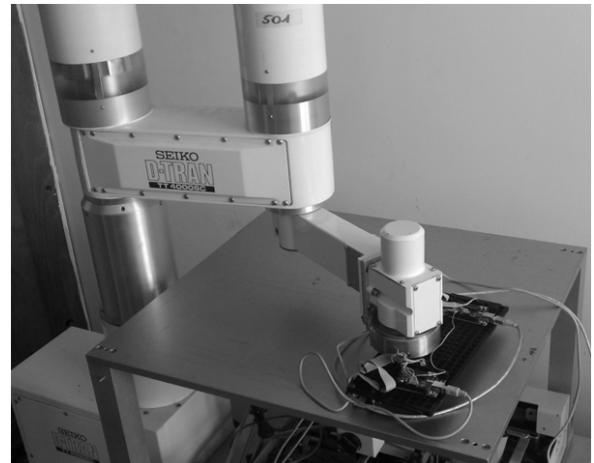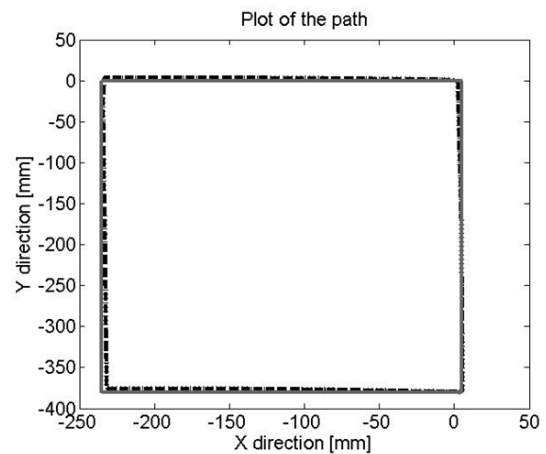

Fig. 9. Measurement with constant orientation

mm eccentricity. This offset caused about 5 mm error at the change of the orientation on the edges of the rectangle, because in this case the TCP of the optical flow moved on an arc. See Fig. 11.

4 SENSOR CORRELATION AND CREDIBILITY

The motion of the robot can be measured with three methods as it is described above. The proposed methods and the sensor fusion are implemented in an embedded system to give position and orientation feedback for the robot control. In this method the credibility is the weight of the measured parameter in the equations of the sensor fusion. The block diagram of the implementation can be seen at Fig. 12, where the parameters are the following:

1. $x_{ref}, y_{ref}, \varphi_{ref}$ are the position and angular position references in robot coordinate system
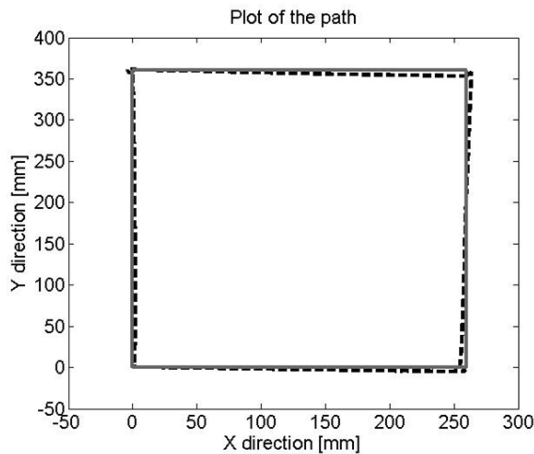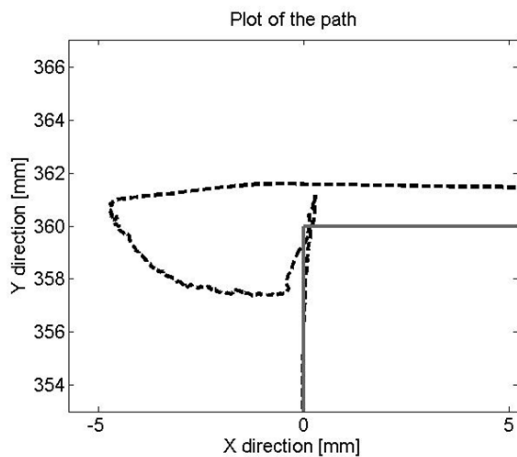
Fig. 10. Measurement with different orientations

Fig. 11. Offset problem

2. x, y, φ are the position and the angular position of the robot

3. $\tilde{x}$, $\tilde{y}$, $\tilde{\varphi}$ are the estimated position and the estimated angular position of the robot

4. ω_1, ω_2, ω_3 are the angular positions of the wheels

5. $\ddot{x}$, $\ddot{y}$, $\ddot{z}$ are the accelerations of the robot

6. x, y, φ are the position and the angular position of the robot

7. ρ, ϕ, θ are the angular position of the robot

8. $\dot{\rho}, \dot{\phi}, \dot{\theta}$ are the angular velocities of the robot

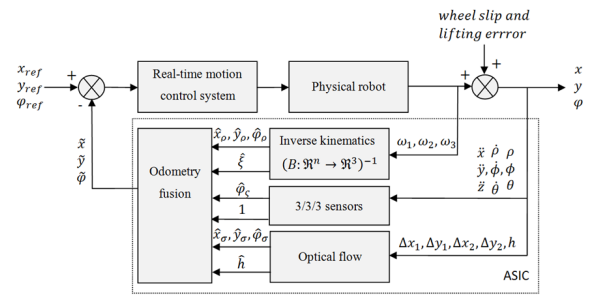9. Δx_1, $\Delta y_1, \Delta x_2$, Δy_2 are the position changes in sensor coordinate systems

Fig. 12. System block diagram

10. h is the sensor height and $\hat{h}$ is the credibility of the odometry sensor

11. $\hat{x}_\rho$, $\hat{y}_\rho$, $\hat{\varphi}_\rho$ are the position and the angular position of the robot calculated from the inverse kinematics

12. $\hat{x}_\sigma$, $\hat{y}_\sigma$, $\hat{\varphi}_\sigma$ are the position and the angular position of the robot calculated from the optical flow sensors

13. $\hat{\varphi}_\xi$ is the estimated angular position of the robot calculated from the 3/3/3 sensor fusion

14. $\hat{\xi}$ is a credibility parameter estimated by the inverse kinematics

The mobile robot can be controlled similarly to many industrial machines like CNC-s, milling machines and manipulators, where the path planning method calculates the references for the servo amplifiers and there is no feedback for the central controller. In this configuration -in case of any fault in a joint- the servo amplifier generates an error signal and the central controller disables the whole machine. The designed embedded system is synchronized with the real-time motion controller of the robot and provides position and angular position feedback for the system. The motion control and the position feedback runs at 1 kHz cycle time so the time constant of the controller is much lower than the mechanical time constant. The $\hat{x}_\rho$, $\hat{y}_\rho$, $\hat{\phi}_\rho$ and $\hat{\xi}$ values of the inverse kinematics module can be calculated on this frequency, where- $\hat{\xi}$ is an estimated credibility parameter, which comes from the unexpected events of the motion like follow error, motor current, wheel accelerations ($\ddot{\omega}_1$, $\ddot{\omega}_2, \ddot{\omega}_3$). All the methods (inverse kinematics, 3/3/3 sensor, optical flow) have credibility, and they are related to each other. The orientation comes from the 3/3/3 sensor, which has constant credibility. The value of- $\hat{\xi}$ and- $\hat{h}$ were defined and validated during measurements and the values can be equal to one, higher than one and lower than one. For example in ideal circumstances the credibility of all the methods would be equal. In line with the fusion of the estimated values, different special rules can be defined to handle unexpected

circumstances like wheel scraping, magneto meter problems near electrical machines in buildings, dirty optical flow sensors, etc. [20, 21].

During the credibility based fusion of the estimated values another problem came from the different time constants of the 3/3/3 sensor, the optical flow feedback loops and the motion control loop. The optical flow sensors and the 3/3/3 sensors data registers are read at 50Hz sampling rate but the kinematics runs at 1 kHz. According to the different time constants 3/3/3 sensor and optical flow method have recursive filters to avoid sudden transitions in the real-time position feedback loop. From the 50 Hz cycle time of the 3/3/3 sensor the time constant of the filter is 20 ms, which is acceptable according to the mechanical time constant of the approximately 40 kg robot. The estimated parameters of the robot odometry ($\tilde{x}$, $\tilde{y}$, $\tilde{\varphi}$) can be expressed as (4.1-4.3).

$$\tilde{x} = \frac{\hat{x}_\rho \hat{\xi} + \hat{x}_\sigma \hat{h}}{\hat{\xi} + \hat{h}} \tag{30}$$

$$\tilde{y} = \frac{\hat{y}_\rho \hat{\xi} + \hat{y}_\sigma \hat{h}}{\hat{\xi} + \hat{h}} \tag{31}$$

$$\tilde{\varphi} = \frac{\hat{\varphi}_\rho \hat{\xi} + \hat{\varphi}_\xi 1 + \hat{\varphi}_\sigma \hat{h}}{\hat{\xi} + 1 + \hat{h}} \tag{32}$$

The credibility of the robot odometry ($\hat{\xi}$) can be tuned with experimental results and can be dependent from different motion related parameters as equation (33).

$$\hat{\xi}(k_1 \frac{\Delta t_{cont}}{\Delta i_1{}^2 + \Delta i_2{}^2 + \Delta i_3{}^2}, k_2 \frac{\Delta t_{cont}}{\ddot{\varphi}_1^2 + \ddot{\varphi}_2^2 + \ddot{\varphi}_3^2}, \dots) \tag{33}$$

where k_1 and k_2 are constant parameters to optimize the function, Δi_n are the motor currents, $\ddot{\varphi}_1$ are the angular accelerations of the wheels and Δt_{cont} is the motion control time period. With a fine tuning these methods could filter the unexpected dynamical events like wheel slipping. During the experiments, the odometry credibility was resulted from the change of the motor currents. The credibility of the robot odometry sensor ($\hat{h}$) can be expressed as equation (34).

$$\hat{h} = k \frac{1}{h_1{}^2 + h_2{}^2} \cdot \frac{S_{QUAL}}{40} \tag{34}$$

where k is constant to optimize the exponential function, S_{QUAL} is the surface register of the sensor, 40 is the reference value of the S_{QUAL} register in case of white paper, h_1 and h_2 are the distances between the sensors and the ground plane (surface). According to the sensor datasheet, it measures from 3.4 mm without any problems but during the experiments we could use the sensors even around 10 mm distance. For the experimental results $k = 200$ where used. For example in case of a 10 mm distance at

each sensors and the S_{QUAL} register is 100 and the odometry measurement still works so $\hat{h} = 1$. Over 10 mm and $S_{QUAL} < 40$ the result can be $\hat{h} \ll 1$, under 10 mm and $S_{QUAL} > 40$ the result can be $\hat{h} \gg 1$.

The real-time motion controller contains a path planner, an interpolation between the position and the angular position and three PD controllers for the wheels. During the robot motion the following constant parameters can be tuned:

1. maximal velocity and angular velocity of the robot

2. maximal acceleration and angular acceleration of the robot

3. maximal angular velocity of the wheels

4. maximal angular acceleration of the wheels

5. *P* and *D* parameters of the wheel position controllers [22]

5   OPEN LOOP TEST

To prove the concept several open loop tests were made on the robot. In this case the embedded system measured the robot position and orientation during motion on a reference path. The grey path lines on the graphs are measured by the embedded system, the points are the initial and the final points of the path which are measured by a motion capture system and the dotted black line is the path, which was performed for the motion (reference).

The most accurate measurement (initial point and final point) of the robot position was made with the existing motion capture system of the Mechatronics, Optics and Mechanical Engineering Informatics Department of Budapest University of Technology and Economics. [23] The motion capture system could not calculate real-time the motion of the robot with the requested resolutions so we could use only the initial and the last points of the motion.

For the first time the orientation of the robot did not change during the motion Fig. 13. ($\Delta\varphi_{robot}(t) = 0$) -In this case the position error was only around 20 millimeters at the end of the path Fig. 14.

For the second time the motion and the robot orientation were always parallel with the direction of the motion Fig. 15. ($\Delta\varphi_{robot}(t) \neq 0$) In this case the error was around 220 millimeters at the end of the path Fig. 16.

The distance between the real end position and the expected end position of the robot showed the same results as the last values of the error plots, which can be compensated during path planning [24-26].
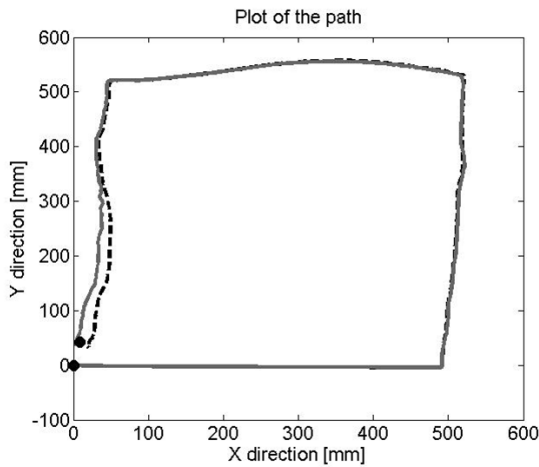
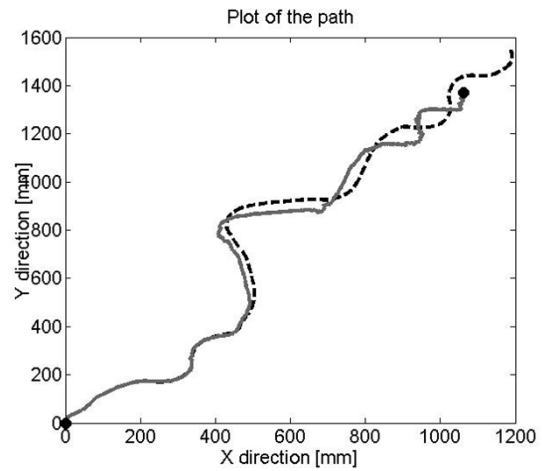*Fig. 13. Open loop test one with constant orientation*

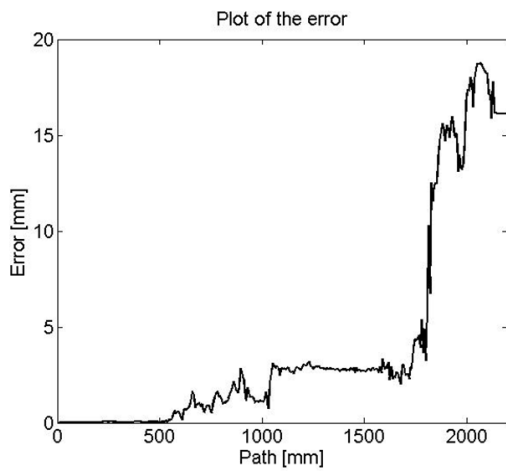*Fig. 15. Open loop test two with different orientations*

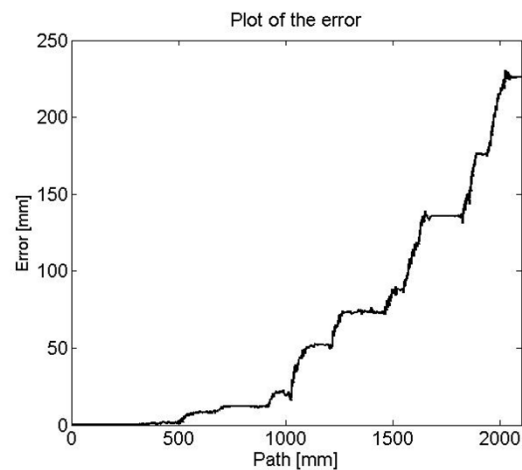*Fig. 14. Open loop test one position error*

Fig. 16. Open loop test two position error

6   CONCLUSION

During motion, the kiwi drive in Ethon continuously accumulated the position and the orientation errors. This paper described an implemented solution for kiwi drive position and orientation problem. The proposed method is based on the inverse kinematics, a sensor fusion between magnetometer, accelerometer, and gyroscope and on a mouse sensors based optical flow system. The mouse sensor measurements and the open loop test proved that the concept can improve the navigation of a kiwi drive based holonomic mobile robot. Refocusing the optics of the mouse sensor based system the accuracy can be further improved. The increasing market and needs of the service robot sector require easy-to-implement and low cost solutions in mobile robotics. By the embedded system based service robots with limited calculation throughput the indoor localization is an ongoing problem.

REFERENCES

[1] Hakyoung Chung, Lauro Ojeda, Johann Borestein, "Sensor fusion for Mobile Robot Dead-reckoning With a Precision-calibrated Fiber Optics Gyroscope", in *International Conference on Robotics & Automation*, (Seoul, Korea), May 21-26, 2001, pp. 3588-3593.

[2] Munir Zaman, "High Precision Relative Localisation Using a Single Camera", in *IEEE International Conference on Robotics and Automation*, (Roma, Italy), April 10-14, 2007, pp. 3908-3914.

[3] S. Nandy, S. N. Shome, R. Somani, T.Tanmay, G. Chakraborty, C. S. Kumar, "Detailed Slip Dynamics for Nonholonomic Mobile Robotic System", in *IEEE International Conference on Mechatronics and Automation*, (Beijing, China), August 7-10, 2011, pp. 519-524.

[4] Yuan Ping Li, Marcelo H. Ang Jr, Wei Lin, "Slip Modelling, Detection and Control for Redundantly Actuated Wheeled Mobile Robots", in *IEEE/ASME International Conference on Advanced Intelligent Mechatronics*, (Xi'an, China), July 2-5, 2008, pp. 967-972.

[5] Chris C. Ward, Karl Iagnemma, "Model-Based Wheel Slip Detection for Outdoor Mobile Robots", in *IEEE International Conference on Robotics and Automation*, (Roma, Italy), April 10-14, 2007, pp. 2724-2729.

[6] Jongdae Jung, Hyoung-Ki Lee, Hyun Myung, "Fuzzy-Logic-Assisted Interacting Multiple Model (FLAIMM) for Mobile Robot Slip Compensation", in *IEEE World Congress on Computational Intelligence*, (Brisbane, Australia), June, 10-10, 2012, pp. 1-8.

[7] Kovács B., Szayer G., Tajti F., Korondi P. Nagy I., "Robot with Dog Type Behaviour", *EDPE 2011*, pp. 4-5

[8] Ferenc Tajti, Géza Szayer, Bence Kovács, Péter Korondi, "Robot base with holonomic drive", in *19th World Congress of the International Federation of Automatic Control (IFAC 2014)*, (Capetown, South Africa), August, 2014, pp. 11-16.

[9] Hyoung-Ki Lee, Kiwan Choi, Jiyoung Park, Yeon-Ho Kim, Seokwon Bang , "Improvement of Dead Reckoning Accuracy of a Mobile Robot by Slip Detection and Compensation using Multiple Model Approach", in *IEEE/RSJ International Conference on Intelligent Robots and Systems*, (Nice, France), September 22-26, pp. 1140-1147.

[10] Xiaojing Song, Lakmal D Seneviratne, Kaspar Althoefer, Zibin Song, "A Robust Slip Estimation Method for Skid-Steered Mobile Robots", in *Intl. Conf. on Control, Automation, Robotics and Vision*, (Hanoi, Vietnam), December 17-20, 2008, pp. 279-284.

[11] Isaku Nagai, Keigo Watanabe, Keiji Nagatani, Kazuya Yoshida, "Noncontact Position Estimation Device with Optical Sensor and Laser Sources for Mobile Robots Traversing Slippery Terrains", in *IEEE/RSJ International Conference on Intelligent Robots and Systems*, (Taipei, Taiwan), October 18-22, 2010, pp. 3422-3427.

[12] Alberto Olivares, Gonzalo Olivares, J. M. Gorriz, J. Ramirez, "High-Efficiency Low-Cost Accelerometer-Aided Gyroscope Calibration", in *International Conference on Test and Measurement*, 2009, pp. 354-360.

[13] Andrea Bonarini, Matteo Matteucci, Marcello Restelli, "Automatic Error Detection and Reduction for an Odometric Sensor based on Two Optical Mice", in *IEEE International Conference on Robotics and Automation*, (Barcelona, Spain), April, 2005, pp. 1675-1680.

[14] Csaba Szász, Géza Husi "Novel multimodal communication skills implementation on the NI-9631 robot" in Proceedings of the IECON 2013: 39th Annual Conference of the IEEE Industrial Electronics Society 2013. pp. 7837-7842.

[15] A. Rojko and K. Kozlowski, Lifelong Education in Robotics and Mechatronics, Methods and Models in Automation and Robotics (MMAR), 2012, pp. 343-348, DOI: 10.1109/MMAR.2012.6347865

[16] Andrea Bonarini, Matteo Matteucci, Marcello Restelli, "A Kinematic-independent Dead-reckoning Sensor for Indoor Mobile Robotics", in *IEEE/RSJ International Conference on Intelligent Robots and Systems*, (Sendai, Japan), September 28- October 2, 2004, pp. 3750-3755.

[17] Ping-Lin Wu, Shyr-Long Jeng, Wei-Hua Chieng, "Least Squares Approach to Odometry based on Multiple Optical Mouse Sensors", in IEEE Conference on Industrial Electronics and Applicationsis, 2010, pp. 1574-1578.

[18] Robert Ross, John Devlin, Song Wang, "Toward Refocused Optical Mouse Sensors for Outdoor Optical Flow Odometry", in *IEEE SENSORS JOURNAL*, June, 2012, Vol. 12, No. 6, pp. 1925-1932.

[19] Mauro Cimino, Prabhakar R. Pagilla, "Location of optical mouse sensors on mobile robots for odometry", in *IEEE International Conference on Robotics and Automation*, (Anchorage, Alaska, USA), May 3-8, 2010, pp. 5429-5434.

[20] Cristina Tar in Sauer, Hermann Brugger, Eberhard P .Hofer, Bernd Tibken, "Odometry Error Correction by Sensor Fusion for Autonomous Mobile Robot Navigation", in *IEEE Instrumentation and Measurement Technology Conference*, (Budapest, Hungary), May 21-23, 2001, pp. 1654-1658.

[21] Géza Husi, Péter Szemes "Control of NI SbRIO-9631 Prototype Robot on the Basis of Hand Movement" in 10th IFAC Symposium on Robot Control 2012 : (SYROCO 2012, Dubrovnik, Croatia,) Sept. 5-.7, 2012. pp. 859-869.

[22] Csaba Budai, László L. Kovács, "Limitations Caused by Sampling and Quantization in Position Control of a Single Axis Robot", *OWD 2013, XV International PhD Workshop*, (Gliwice, Poland), October 19-22, 2013, pp. 466-471. ISBN: 978-83-935427-2-1

[23] Devecseri V, Dóka A, Molnár J, Tamás P, An Ethological Motion Capture System, in 12th IEEE International Symposium on Computational Intelligence and Informatics, CINTI November, 2011, Budapest, Hungary, IEEE Press 2011, pp. 487-491. DOI: 10.1109/CINTI.2011.6108555

[24] Wataru Maebashi, Kazuaki Ito, Makoto Iwasaki, "Practical Feedback Controller Design for Micro-Displacement Positioning in Table Drive Systems", in *AUTOMATIKA 54(2013) 1, 9–18*, Online ISSN 1848-3380, Print ISSN 0005-1144, pp. 9-18.

[25] Robert Ross, John Devlin, "Analysis of Real-Time Velocity Compensation for Outdoor Optical Mouse Sensor Odometry", in *11th Int. Conf. Control, Automation, Robotics and Vision*, (Singapore), December 7-10, 2010, pp. 839-843.

[26] Domokos Kiss, Gábor Tevesz, "Nonholonomic Path Planning for a Point Robot with Car-Like Kinematics", in *Periodica Polytechnica, Electrical Engineering and Computer Science*, (Budapest, Hungary), 2013, vol. 57, no. 3, pp. 65-76, doi: 10.3311/PPee.2099

F. Tajti received MSc. in 2012 at Mechatronics at Budapest University of Technology and Economics. Since then he is Ph.D. student at the Department of Mechatronics Optics and Mechanical Engineering Informatics in the Faculty of Mechanical Engineering. During his engineering school he got several Scientific Student Conference awards. Since 2012 he is working in the MTA-ELTE Comparative Ethological Research Group (MTA 01 031) of the Hungarian Academy of Sciences. During his whole professional carrier he worked on or even coordinated several engineering project in the field of industrial robot control and mobile robotics. He developed for the Narvik University College in Norway, for the Institute for Computer Science and Control of the Hungarian Academy of Sciences.

G. Szayer received MSc. in 2011 at Mechatronics at Budapest University of Technology and Economics (BME). During his engineering school he got several Scientific Student Conference awards: two first-, and three second- and more other prices. He worked 1.5 years in the Budapest R&D Center of Knorr-Bremse as a function development embedded software engineer before applying to the PhD course of the Department of Mechatronics Optics and Engineering Informatics at the Faculty of Mechanical Engineering of BME. He founded his own company – General Mechatronics Ltd. – in 2012 with Bence Kovacs, and works on different industrial and R&D projects in the field of industrial- and mobile robotics.

B. Kovacs received MSc. degree in 2011 at Mechatronics at Budapest University of Technology and Economics. During his engineering school he got several Scientific Student Conference awards: two first-, and three second- and more other prices. Before applying to PhD course of the Department of Mechatronics Optics and Engineering Informatics at the Faculty of Mechanical Engineering of BME, he worked two years in the Budapest R&D Center of Ericsson. Within this time, he worked as software developer then worked as hardware developer of high speed network systems. He founded his own company – General Mechatronics Ltd. – in 2012 with Géza Szayer, and works on different industrial and R&D projects in the field of industrial- and mobile robotics.

P. Barna received BSc in 2013 at Mechatronics at Budapest University of Technology and Economics, and is now an MSc student. There he became interested and involved in the theoretical background of mobile robotics. He also plans to be a PhD student in the field of mobile robotics related computer vision. During the last two semesters he worked on project Ethon at the Department of Mechatronics, Optics, and Engineering Informatics Budapest University of Technology and Economics especially on the theoretical part and the implement of the optical flow method. He also works for a small firm specialised in machine vision solutions.

P. Korondi (M'98-SM'11) received the Dipl. Eng. and Ph.D. degrees in electrical engineering from the Technical University of Budapest, Budapest, Hungary, in 1984 and 1995, respectively. Since 1986, he has been with Budapest University of Technology and Economics (formerly the Technical University of Budapest). From April 1993 to April 1995, he worked in the laboratory of Prof. Harashima and Prof. Hashimoto at the Institute of Industrial Science, The University of Tokyo, Japan, where he continues to spend a month each year, working on joint research. As a result of this cooperation, the Intelligent Integrated System Japanese–Hungarian Joint Laboratory was founded in 2001. His research interests include telemanipulation and motion control. Dr. Korondi is a founding member of the International PEMC Council. He is also with the MTA-BME Control Engineering Research Group of the Hungarian Academy of Sciences.

AUTHORS' ADDRESSES

Ferenc Tajti, M.Sc.
Géza Szayer, M.Sc.
Bence Kovács, M.Sc.
Péter Barna, M.Sc.
Prof. Péter Korondi, Ph.D
Department of Mechatronics, Optics and Engineering Informatics,
Faculty of Mechanical Engineering,
Budapest University of Technology and Economics,
1521 Budapest, Pf. 91., Hungary
email: tajti, geza.szayer, bence.kovacs, barna,
korondi@mogi.bme.hu